Adsorption 6, 241–249, 2000

A Grand Canonical Monte-Carlo Simulation Study of Xenon Adsorption in a Vycor-like Porous Matrix

R.J.-M. PELLENQ, S. RODTS, V. PASQUIER, A. DELVILLE AND P. LEVITZ
Centre de Recherche sur la Matière Divisée, CNRS et Université d'Orléans, 1b rue de la Férollerie, 45071 Orléans, cedex 02, France
pellenq@cnrs-orleans.fr

Received June 15, 1999; Revised March 21, 2000; Accepted April 14, 2000

Abstract. We have performed atomistic Grand Canonical Monte-Carlo (GCMC) simulations of adsorption of xenon in a Vycor-like matrix at 195 K. The disordered mesoporous network is obtained by applying a numerical 3D off-lattice reconstruction procedure to a simulation box originally containing silicon and oxygen atoms of a non-porous silica solid. In order to reduce the computational cost, we have applied a homothetic decrease of the simulation box dimensions which preserves the morphology and the topology of the pore network (the average pore dimension is then around 30 Å). The surface chemistry is obtained in a realistic fashion by saturating all dangling bonds with hydrogen atoms. Small angle scattering spectra calculated on different numerical samples have evidenced a departure from Porod's law due to surface roughness. The simulated isotherms calculated on such disordered connected porous networks, show the capillary condensation phenomenon. The shape of the adsorption curves differs from that obtained for simple pore geometries. The analysis of the adsorbed quantity distribution indicates partial molecular-film formation depending on the local surface curvature and roughness.

Keywords: silica glasses, CPG, Vycor, adsorption, capillary condensation, molecular simulation, Monte-Carlo, SANS, SAXS, fractals, surface roughness, Porod's law, Gurvitch rule, hysteresis loop

1. Introduction

Disordered porous solids play an important role in industrial processes such as separation, heterogeneous catalysis, etc... The confinement and the geometrical disorder strongly influence the thermodynamics of a fluid adsorbed inside the porous network. This raises the challenge of describing the morphology and the topology of these porous solids (Levitz et al., 1997). A structural analysis can be achieved by using optical and electron microscopy, molecular adsorption, etc... Correlations at different length scales of the solid parts in the overall structure can be obtained from small angle scattering. It is well known that density fluctuations are at the origin of scattering: in a porous matrix, these fluctuations are located at the interface between voids and solid regions. Vycor is a porous silica glass which is widely used as a model structure for the study of the properties of confined fluids in mesoporous materials. The pores in Vycor have an average radius of about 35 Å (assuming a cylindrical geometry) and are spaced about 200 Å apart (Agamalian et al., 1997; Page et al., 1995).

Provided that the adsorption experiment is run at a temperature lower than the critical capillary temperature (T_{cc}), the adsorption theory for an *infinite* cylinder or slit with no external surface, predicts an adsorption isotherm characterized by a discontinuity: the well-known capillary condensation (Ball and Evans, 1989; Peterson and Gubbins, 1987). Since adsorption and desorption branches do not superimpose, capillary condensation below T_{cc}, is also characterized by a hysteresis loop; the critical capillary condensation temperature is therefore defined as the temperature for which the hysteresis loop disappears. During adsorption, at pressures higher than that corresponding to the

hysteresis closure point (thus at $T < T_{cc}$), the adsorbed molecular film is in a metastable state and misses out the transition to its true free energy minimum: the system does not have fluctuation of sufficient amplitude to probe and find the equilibrium state (free energy barrier) (Celestini, 1997). Statistical thermodynamics indicates that there is no particular reason for capillary evaporation to occur at equilibrium although it is usually assumed to be the case in pore size distribution calculation methods (Rouquerol et al., 1998). At $T > T_{cc}$, the reversible adsorption/desorption isotherm curve increases monotonically with no discontinuity. For a given adsorbate, the smaller the pore width, the lower the critical capillary temperature (T_{cc} is always lower than that of the bulk homogeneous phase). In the pores of MCM41 (an ordered mesoporous silica) with radius less than 18 Å, no capillary transition is observed for nitrogen at 77 K, the capillary critical temperature being estimated for such a pore width to be less than 68 K (Morishige et al., 1997) ($T_c(N_2, \text{bulk}) = 126.2$ K). The existence of the capillary condensation phenomenon through its dependence upon the pore size states the frontier between the *meso* and the *micro*-porosity: in a micropore, a fluid cannot undergo a capillary (first order) transition. In other words, a fluid confined in a micropore is always in supercritical conditions whatever the temperature. From a physical point of view, first-order capillary transition cannot occur in micropores because (i) fluid molecules in such environment are confined in the strong potential field of the solid matrix compare to the fluid-fluid energy and (ii) the small number of neighbors due to the reduced confining space, prevent any cooperative effect.

The capillary condensation theory has been validated with simulation on simple geometries (slits and cylinders) (Peterson and Gubbins, 1987; Bojan and Steele, 1996) and experiments on MCM41 samples of different diameters (Morishige et al., 1997). It is important to note MCM41 materials are, to our knowledge, the only mesoporous structures having a well-defined pore geometry; the rest of the mesoporous solids being characterized by a collection of connected pores of different sizes and shapes. For those disordered materials, the condensation/evaporation hysteresis loop can be also explained on the basis of the percolation theory: during desorption, a given pore filled with condensate has to be connected to a larger pore already filled with gas in order to undergo its (local) capillary evaporation (Mason, 1988). Desorption occurs when the set of pores filled with gas constitutes a percolation network connected to the outer surface of the mesoporous sample. The evaporation delay giving rise to the hysteresis loop, is then the consequence of pore constrictions and bottle necks geometries. However, there is no experimental evidence of the percolation process while the "metastable-state" theory is found to give a good account of experimental observation in systems such as MCM41. Therefore in the case of disordered mesoporous materials, the determination of the adsorption/desorption mechanism from a simple analysis of isotherms is a difficult task since it may result from "single tube" behaviors competing networking effects. The aim of this work is to provide an insight in the adsorption mechanism in a disordered connected mesoporous medium such as vycor at a microscopic level.

2. Simulation Procedure

2.1. Generating Vycor-like Numerical Samples

We have used on an off-lattice reconstruction algorithm in order to numerically generate a porous structure which has the main morphological and topological properties of real vycor in terms of pore shape and connectivity. One challenge was to define a realistic mesoporous environment within the smallest simulation box. In a previous study, it has been shown that chord distribution analysis on large non-periodic reconstructed 3D structures of disordered materials allows to calculate small angle scattering spectra. In the particular case of Vycor, the agreement with experiment is good: on a box of several thousands Å in size, the calculated curve exhibits the experimentally observed correlation peak at 0.026 $Å^{-1}$ (Levitz and Tchoubar, 1992). The first criterium that our minimal reconstruction has to meet is to reproduce this correlation peak in the diffuse scattered intensity spectrum which corresponds to a minimal (pseudo) unit-cell size around 270 Å. However such a simulation box size still remains too large to be correctly handled in an atomistic Monte-Carlo simulation of adsorption. This is the reason why we have applied an homothetic reduction with a factor of approximately 2.54 so that the final numerical sample is contained in a box of about 107 Å in size (see below). This transformation preserves the pore morphology but reduces the average pore size from 70 Å (as reported for 7930 Corning Vycor) to roughly 30 Å. As a further consequence, the pore spacing, originally at 200 Å, decreases to 75 Å. Note that a reconstructed minimal numerical sample is still well within the mesoporous

domain that the homethetic reduction does not create micropores i.e. cavities smaller than 4–5 adsorbate diameters. The atomistic pseudo-Vycor porous medium has been obtained by applying the off-lattice functional to a box containing the silicon and oxygen atoms of 15^3 unit cells of cubic cristoballite (a siliceous nonporous solid). This allows to cut out portions of the initial volume in order to create the Vycor porosity. The off-lattice functional represents the gaussian field associated to the volume autocorrelation function of the studied porous structure (Levitz, 1998). This approach encompasses a statistical description: it allows to generate a set of morphologically and topologically equivalent numerical 3D samples. Periodic boundary conditions are applied in order to simplify the Grand Canonical Monte-Carlo (GCMC) adsorption procedure. In fact, one can considered each sample as being an independent portion of a larger pseudo-Vycor structure. In order to model the surface in a realistic way and to ensure electroneutrality, all oxygen dangling bonds are saturated with hydrogen atoms (all silicon atoms in an incomplete tetrahedral environment are removed). The gradient of the local gaussian field allows to place each hydrogen atom in the pore void perpendicular to the interface at 1 Å from the closest unsaturated oxygen: the O─H surface density group is 7 OH per nm^2 (4.81 mmol OH/g) in excellent with experimental values for porous silica glasses (Landmesser et al., 1997).

2.2. *The Grand Ensemble Monte-Carlo Simulation Technique as Applied to Adsorption*

In this work, we have used a PN-type potential function as reported for adsorption of xenon in silicalite (a purely siliceous zeolite): it is based on the usual partition of the adsorption intermolecular energy which can written as the sum of a dispersion interaction term with the repulsive short range contribution and an induction term (no electrostatic interaction in the rare gas/surface intermolecular potential function) (Pellenq and Nicholson, 1994; Pellenq et al., 1996). The dispersion and induction parts in the Xe/H potential is obtained assuming that hydrogen atoms have a partial charge of $0.5e$ ($q_O = -1e$ and $q_{Si} = -2e$ respectively) and a polarizability of 0.58 $Å^3$; the Xe/H repulsive contribution is adjusted on the experimental (vycor) low coverage isosteric heat of adsorption (Qst(0) = 17 kJ/mol) (Burgess et al., 1990). One may infer that the isosteric heat of adsorption at zero coverage on the pseudo-vycor numerical samples should be higher than that measured on the real material due to higher surface curvature induced by the homothetic reduction. In fact, Qst(0) does not depend strongly upon surface curvature for pore larger than 8 Å in size: in the case of the Xe/silicalite-1 zeolite (pore diameter 5 Å), Qst(0) = 27.4 kJ/mol (Pellenq and Nicholson, 1994; Pellenq et al., 1996), it decreases to 17.9 kJ/mol in the cavity of NaY zeolite (pore diameter 8 Å) (Pellenq and Nicholson, 1994; Pellenq et al., 1996). Note that in the last case, Qst(0) is only 1 kJ/mol larger than that in vycor. Therefore, we can safely consider that the isosteric heat of adsorption at zero coverage in our numerical pseudo-vycor samples is that of the real material. The Xe/Xe potential energy was calculated on the basis of a Lennard-Jones function ($\varepsilon = 281$ K and $\sigma = 3.89$ Å) which gives a good fit of the "true" two-body Xe/Xe potential (Barker et al., 1974).

In the Grand Canonical Ensemble, the independent variables are the chemical potential, the temperature and the volume (Nicholson and Parsonage, 1982). At equilibrium, the chemical potential of the adsorbed phase equals that of the bulk phase which constitutes an infinite reservoir of particles at constant temperature. The chemical potential of the bulk phase can be related to the temperature and the bulk pressure. Consequently, the independent variables in a GCMC simulation of adsorption in Vycor are the temperature, the pressure of the bulk gas and the volume of the simulation cell containing the porous sample as defined above. The adsorption isotherm can be readily obtained from such a simulation technique by evaluating the ensemble average of the number of adsorbate molecules. Note that the bulk gas is assumed to obey the ideal gas law. Control charts in the form of plots of a number of adsorbed molecules and internal energy *versus* the number of Monte-Carlo steps were used to monitor the approach to equilibrium. Acceptance rates for creation or destruction were also followed and should be equal at equilibrium. After equilibrium has been reached, all averages were reset and calculated over several millions of configurations (3×10^5 Monte-Carlo steps per adsorbed molecules). In order to accelerate GCMC simulation runs, we have used a grid-interpolation procedure in which the simulation box volume is split into a collection of voxells (Pellenq and Nicholson, 1995). The Xe/Vycor adsorption potential energy is calculated at each corner of each elementary cubes. An energy 10^6 point grid was calculated for each of the numerical samples A cut through a grid is presented in Fig. 1. Such a

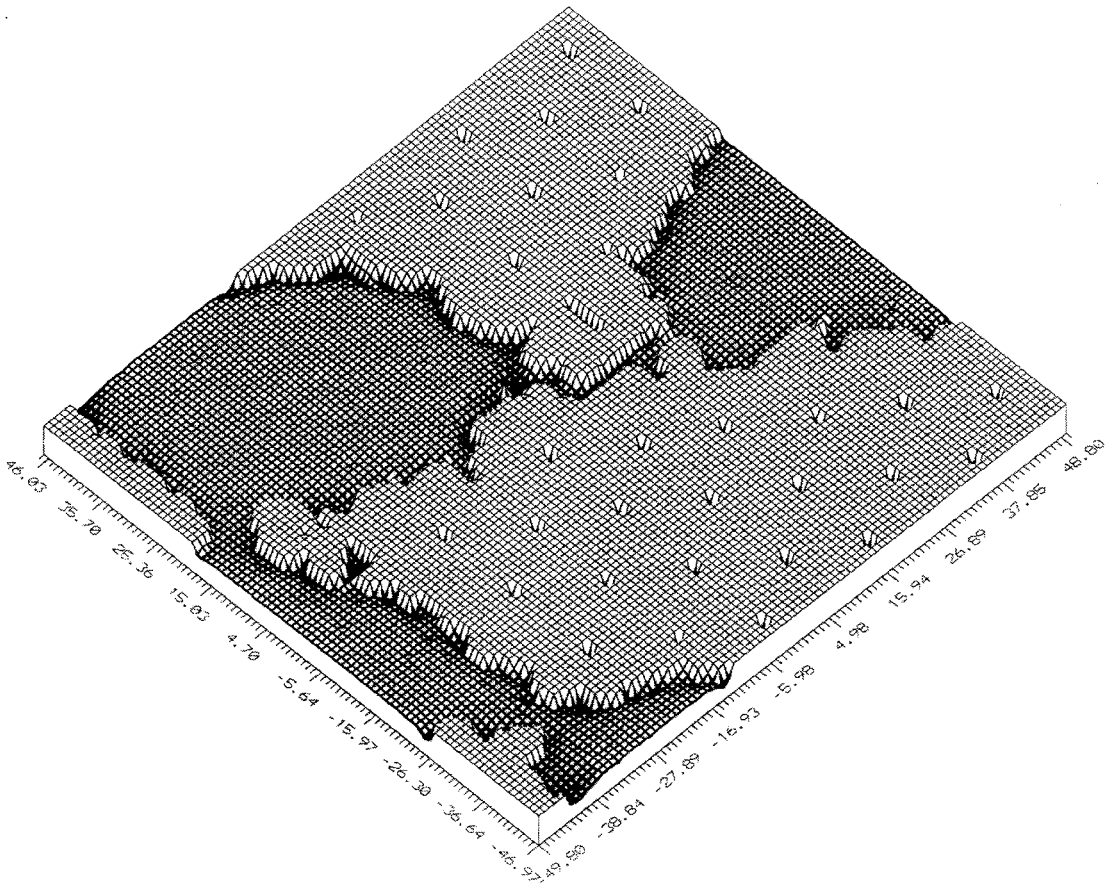

Figure 1. A cut through an energy grid (sample 1). The third (out of plane) dimension corresponds to the adsorbate/surface potential energy: the primary adsorption sites are close to the rough interface (darkest zones).

grid can also be used to obtain the porosity and specific surface (Pellenq and Levitz, to be published). We have found an average specific surface around 200 m^2/g. This value is twice that of the (real) vycor sample used to build up the volume autocorrelation function (from TEM 2D-images) which underlies the off-lattice reconstruction method above outlined (Levitz, 1998). This is one further effect of the homothetic reduction. Note that this is in line with that observed experimentally: the smaller the pore size, the larger the specific surface (Torii et al., 1990).

3. Results and Discussion

3.1. Properties of Pseudo-Vycor Numerical Samples

For all the numerical samples, textural parameters (in terms of porosity and density) are given in Table 1. The porosity ranges from 0.291 to 0.378 while the density ranges from 1.369 to 1.562 g/cm^3. The average density and porosity values are 1.467 g/cm^3 and 0.334 respectively (the values for real vycor are 1.50 g/cm^3 and 0.30). Thus the values of density and porosity of the numerical pseudo-vycor samples are relatively close to that of real vycor. This is not surprising since the off-lattice procedure requires the volume autocorrelation fonction (as obtained from 2D-TEM images) and the porosity of the real material. The density of the final porous samples is simply $(1 - \Phi) * \rho_{silica}$ (ρ_{silica} is the density of bulk silica: 2.2 cm^3/g, Φ is the porosity). Density and porosity exhibit fluctuations that are due to a small-size effect: the numerical reconstruction procedure uses the volume autocorrelation function of (real) vycor as obtained on a *macroscopic* vycor sample. The atomic approach allows the calculation of the small angle-scattering (neutron) spectrum for each sample. They all give very similar diffuse intensity spectra (Fig. 2) with a correlation peak

Table 1. Textural parameters of the different numerical samples of pseudo-vycor (all samples are created within a volume of $(106.95)^3$ Å^3 (rows in bold show the extrema in density and porosity as found from the series of numerical samples). GCMC simulations were run on samples 3 to 7.

Samples	Number of Oxygen atoms	Number of Silicon atoms	Number of Hydrogen atoms	Density (in g/cm^3)	Porosity (%)
1	34079	16453	2346	1.370	0.377
2	35797	17260	2554	1.439	0.347
3	*35987*	*17313*	*2722*	*1.445*	*0.344*
4	***34083***	***16397***	***2578***	***1.369***	***0.378***
5	*38253*	*18498*	*2514*	*1.539*	*0.301*
6	*38435*	*18534*	*2734*	*1.545*	*0.298*
7	***38811***	***18764***	***2566***	***1.562***	***0.291***
8	36347	17600	2294	1.464	0.335

around a mean value at 0.067 Å^{-1}. As for density and correlation peak position around this mean value, reflects the statistical character of the reconstruction procedure. The shift of the correlation peak from 0.026 Å^{-1} (real vycor) to 0.067 Å^{-1} is again a consequence of the homothetic transformation (the ratio $0.067/0.026 = 2.54$ i.e. the homothetic factor). The use of periodic boundary conditions makes impossible any analysis at wave vectors smaller than 0.059 Å^{-1} (which corresponds to the simulation box size). By contrast, larger wave vectors probe distances within the simulation box. The Bragg peaks for wave vectors larger than 1 Å^{-1} are vestiges of the original cubic cristoballite crystal. The decay of the simulated diffused intensity with increasing wave vector is characterized by an algebraic law with exponent equal to -3.5 in good agreement with experiment (Fig. 2) (Levitz et al., 1991; Mitropoulos et al., 1995). This point which holds true for all the numerical samples, deserves more attention. Indeed, it was demonstrated few years ago that the small angle scattering spectrum calculated on a reconstructed 3D sample of vycor with a *smooth* surface shows an algebraic decay with exponent of -4 i.e. obeys the Porod law. Therefore, the departure from the Porod law as observed in for our numerical pseudo-vycor samples, is a consequence of surface roughness which can be estimated on the order of a nanometer i.e. few silicon oxide tetrahedra, in agreement with the energy contour map given in Fig. 1. Therefore, the atomistic approach to porous glass structure as reported in the present work gives a good account of a realistic silica surface roughness. In the particular case of silica glasses, there is no need to invoke any fractal concept to explain the departure from Porod's law (Mitropoulos et al., 1995). Note that the use of the fractal analysis requires several (more than two) length scales (Avnir et al., 1998); this is clearly not the case with silica porous glasses where there are at the most two distinct length scales: one associated to surface roughness

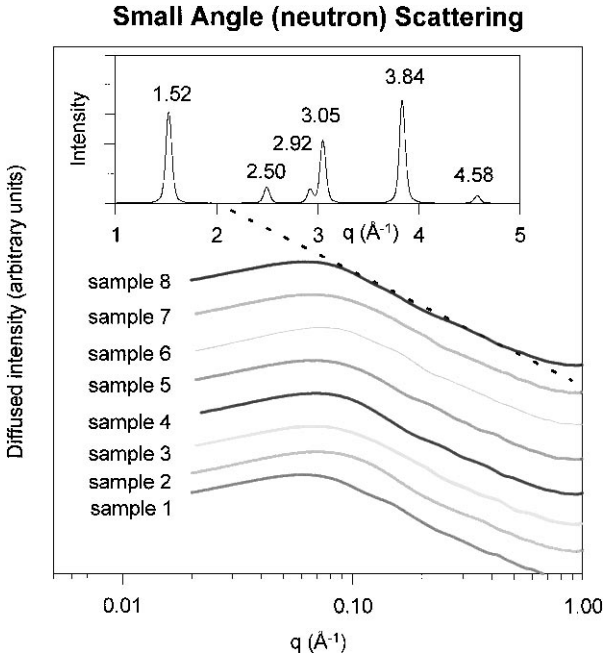

Figure 2. Small Angle (Neutron) Scattering spectra. Insert: diffraction spectrum showing the Bragg peaks of cubic cristoballite (see text) in very good agreement with corresponding (X-ray) experimental peaks that are at 1.515, 2.49, 2.90, 3.03, 3.83 and 4.55 Å^{-1} respectively. The dashed line corresponds to an algebric law of exponent (-3.5) in the region [0.08, 0.2 Å^{-1}] in agreement with experiment (see text).

(few angstroems) and one associated to the pore size distribution (few tenths of angstroems).

3.2. Grand Canonical Monte-Carlo Simulation of Adsorption of Xenon at 195 K

Figure 3 presents the simulated xenon adsorption isotherms on pseudo-vycor samples. They are of type V in the IUPAC classification (Rouquerol et al., 1998). In all cases, capillary condensation is observed: at maximum loading, the fluid density and structure is very close to that of the 3D-liquid at the same temperature (0.0129 Xe/Å^3); this validates the Gurvitch rule (Rouquerol et al., 1998) in the case of xenon adsorption at 195 K. By contrast to that obtained for a single infinite cylinder, the slope at the transition has a finite value. This is in qualitative agreement with experimental studies (Burgess et al., 1974; Nuttal, 1974) and recent Monte-Carlo simulations of nitrogen in disordered porous glasses (Gelb and Gubbins, 1998). Therefore such a behavior can be considered as the signature of *disordered* mesoporous structure. The pseudo-vycor adsorption curves are shifted to the lower pressure region compared to the experimental curve (Burgess et al., 1974; Nuttal, 1974) since the pore size distribution of reconstructed samples is shifted toward a smaller size domain due to the homothetic reduction. We note that all samples exhibit capillary condensation around 45000 Pa. This seems to indicate that the (adsorption) isotherm is not very sensitive to the details of the pore morphology but to a characteristic length which is the mean chord length (Pellenq and Levitz, to be published). At lower pressure, the adsorption isotherms differ from sample to sample; they exhibit inflection points corresponding to *local* condensation in high curvature places of the interface (see below). The average adsorption isotherm given in Fig. 3 is obtained from the arithmetic mean over the 5 sample curves: it qualitatively exhibits the same features. For sample 6, the complete hysteresis loop is also shown in Fig. 3: a sharp (nearly vertical) desorption branch is obtained in agreement with experiment (all simulated curves exhibit the hysteresis loop phenomenon with closure at around 22000 Pa). Since the Grand Canonical Monte-Carlo procedure bypasses all networking percolative effects (the algorithm allows destruction and creation steps anywhere in the pore void without ever requiring them to pass through constrictions), the hysteresis loop as observed in simulation is due to metastable states only in agreement with other simulation results on disordered porous media (Gelb and Gubbins, 1998; Page and Monson, 1996). Furthermore, percolation cannot be envisaged because of the smallness of the numerical samples and the use of periodic boundary conditions. We thus conclude that xenon adsorption/desorption at 195 K is subcritical in such a mesoporous medium. In

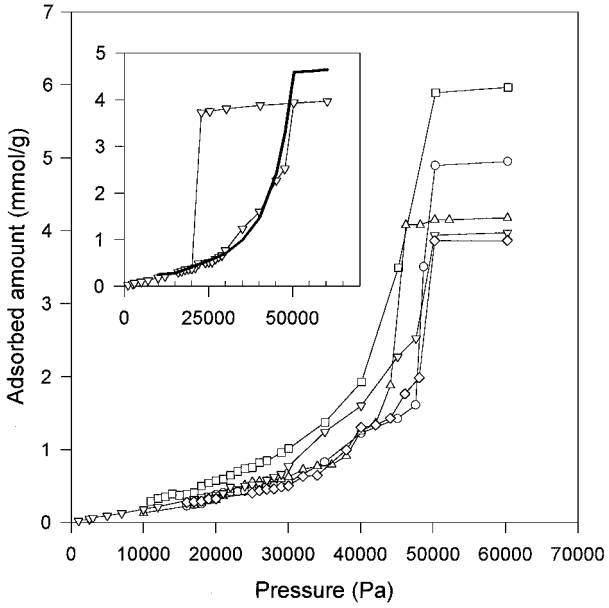

Figure 3. Xe adsorption isotherms at 195 K for numerical pseudo-vycor samples 3 to 7; (circles): sample 3, (squares): sample 4, (up triangles): sample 5, (down triangles): sample 6, (lozanges): sample 7. Differences in the maximum amount adsorbed from sample to sample is due to the fluctuation in porosity (see Table 1 and Fig. 4). The insert shows a complete adsorption/desorption isotherm for sample 6 along with an average adsorption branch (see text).

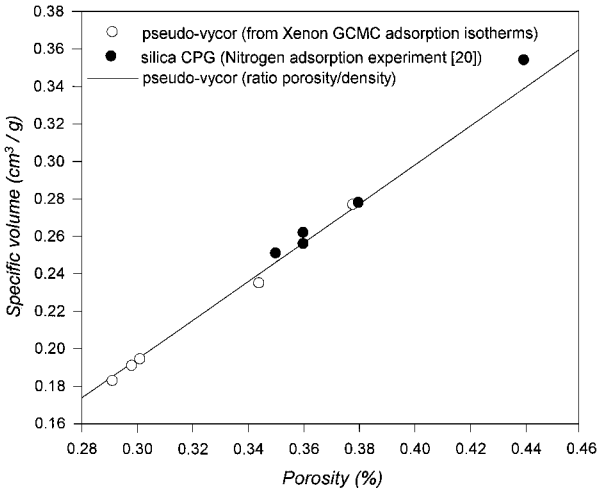

Figure 4. Specific volume versus the matrix porosity (see text).

real vycor, the capillary critical temperature for xenon is estimated at 272.3 K (Ball and Evans, 1989; Burgess et al., 1990; Nuttal, 1974), T_c (bulk) = 289.7 K. It is therefore expected to be less in our case.

Not surprisingly, the theoretical adsorption capacity (specific volume) obtained as the ratio of the porosity with the matrix density for each sample, is a linear function of the porosity in agreement with experiment for series of silica glasses (Torii et al., 1990) (see Fig. 4). Thus, there is a master specific volume *versus* porosity curve for all silica porous glasses. It is interesting to point out that the adsorption capacity of pseudo-vycor numerical samples 5, 6 and 7 is in very good agreement with that of real vycor (as are their values for porosity and density). Figure 4 also shows that the specific volumes as obtained from the various xenon adsorption isotherms presented in Fig. 3 are in good agreement with the theoretical values of the adsorption capacity

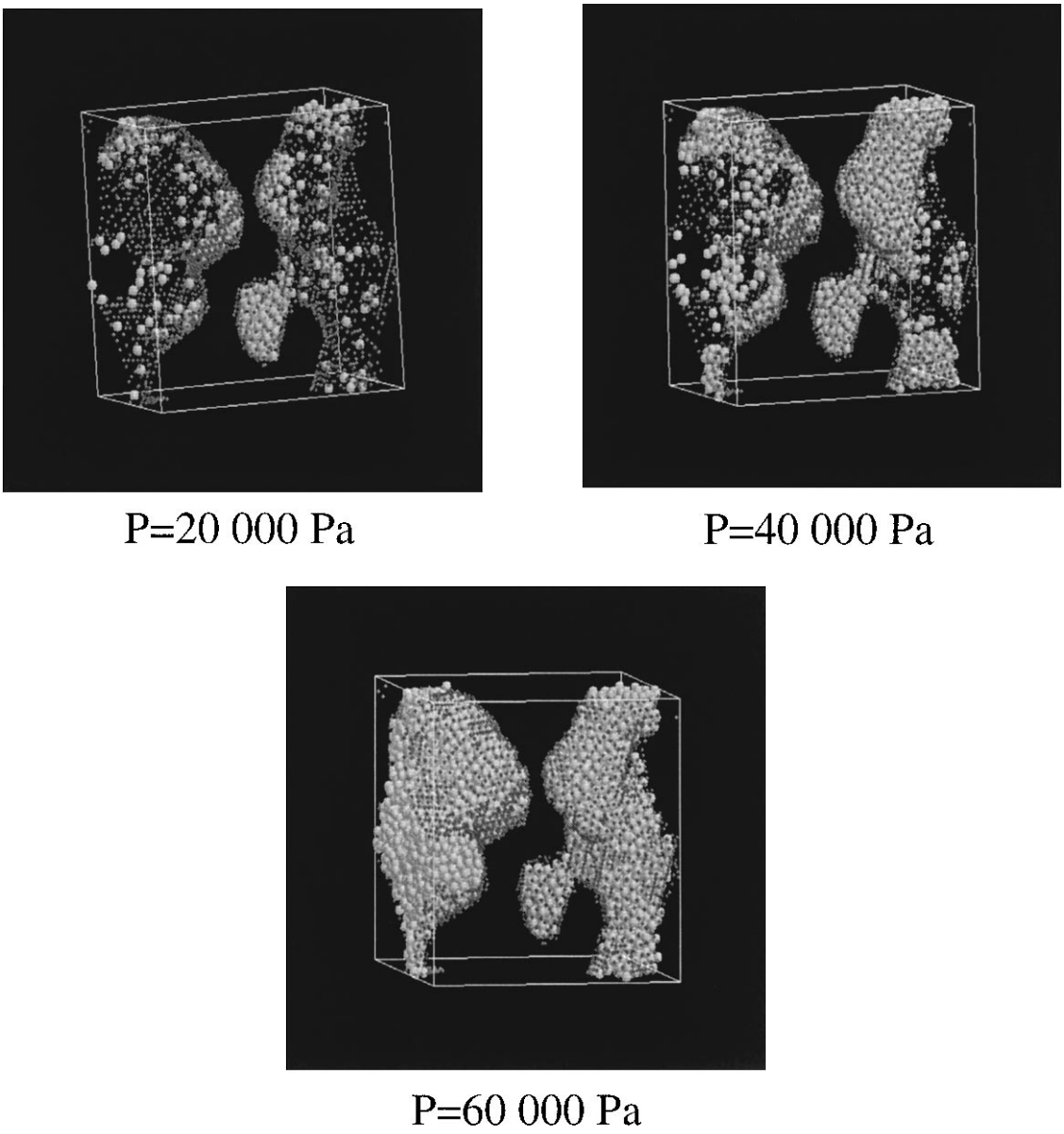

Figure 5. Snapshots for sample 7: $a/P = 20000$ Pa, $b/P = 40000$ Pa, $c/P = 60000$ Pa. One "sees" through the matrix: the dots correspond to the hydrogen atoms which delimitate the interface, the white spheres are xenon atoms.

assuming that xenon condensate has the density of the bulk liquid at the same temperature (2.81 g/cm^3 at 195 K). This implicitly validates the Gurvitch rule (Rouquerol, 1998).

Most important is the adsorption mechanism as deduced from equilibrium configuration snapshots (Fig. 5). At 195 K, xenon does not wet the vycor surface: adsorption and condensation take place in the places of highest surface curvature (this corresponds to regions where the confinement effect is maximum). This leads to an unexpected situation where parts of the pores are filled with condensate while other regions remain uncovered. Therefore, we can infer that monolayer-based method (such as the BET approach) used to determine the specific surface cannot be used in such non-wetting situation for temperatures below the wetting temperature of the confined fluid (since no monolayer film covering the entire surface exists). It is interesting to mention that GCMC simulations of nitrogen adsorption/condensation in similar siliceous glasses have shown that nitrogen at 77 K does form a continuous film on the inner surface (Gelb and Gubbins, 1998). Therefore, one can infer that for a given type of interface (silica in this work), there are a large variety of adsorption behaviours depending on the adsorbate (and probably on the temperature). Note that a similar wetting behavior to that presented in this work has been shown by Monson et al. in a GCMC study of adsorption of a Lennard-Jones fluid in a disordered porous medium characteristic of silica xerogel (Page and Monson, 1996) (an assembly of nanometric silica spheres): it is shown that adsorption and condensation take place in the highest sphere density regions where the confinement effect is maximum: capillary condensation occurs gradually from highest curvature regions to the weakest.

4. Conclusion

We have performed atomistic Grand Canonical Monte-Carlo (GCMC) simulations of adsorption of xenon in a vycor-like matrix at 195 K. This disordered mesoporous network is obtained by using a numerical 3D off-lattice reconstruction method: the off-lattice functional when applied to a simulation box originally containing silicon and oxygen atoms of a non-porous silica solid, allows to create the mesoporosity which has the morphological and the topological properties of the real vycor glass. In order to reduce the computational cost, we have applied a homothetic decrease of the box dimensions which preserves the morphology of the pore network. The surface chemistry is also obtained in a realistic fashion since all dangling bonds are saturated with hydrogen atoms. Small angle scattering spectra calculated on different numerical samples have evidenced a departure from Porod's law which is the consequence of surface roughness. No fractal analysis is needed to interpret such results. The simulated isotherm calculated on such disordered connected porous networks, show the capillary condensation phenomenon accompanied with hysteresis upon desorption in agreement with experiment. The shape of the adsorption curves differ from that obtained for simple pore geometries (slits and cylinders). The analysis of the adsorbed quantity distribution indicates partial wetting depending on the local surface curvature and roughness (wetting should understood in this work as the formation of continuous molecular film at the interface). This leads to an interesting situation in which, parts of the porous network are already filled with liquid while other regions remain only partially covered with an adsorbate film. The smallness of the numerical samples and the way of handling destruction steps in the Monte-Carlo procedure impede a test of percolative aspects of desorption phenomenon often used to explain hysteresis. Recently, Kierlick et al. (1998) have put forward a quenched-annealed lattice gas model in order to represent a fluid confined in a disordered porous material (porosity ~ 0.8): a statistical theory of liquids combined with the replica concept allows to derive a complete phase diagram for the confined fluid. In particular, this model reproduces the lowering of the critical temperature due the confinement. An interesting feature is the occurence of a pre-capillary condensation transition for some values of the y parameter defined as the ratio of the adsorbate-solid potential energy parameters with that of adsorbate-adsorbate interaction. Such a pre-condensation transition has also found in GCMC simulation of Monson et al. (Page and Monson, 1996) in the case of xerogel with porosity around 0.6. It will be very interesting in a future work to check if the pre-capillary condensation phenomenon can be observed in lower porosity systems such as our pseudo-vycor samples.

Acknowledgments

Dr. P. Monson (UMAS, USA), Prof. L. Gelb (University of Florida, USA), Dr. G. Tarjus and Dr. M.-L. Rosinberg (University of Paris VI, France) are

gratefully acknowledged for very stimulating discussions. We also thank the Institut du Développement et des Ressources en Informatique Scientifique, (CNRS, Orsay, France) for the computing grant 98/99281.

References

Agamalian, M., J.M. Drake, S.K. Sinha, and J.D. Axe, "Neutron Diffraction Study of the Pore Surface Layer of Vycor Glass," *Phys. Rev. E*, **55**, 3021–3027 (1997).

Avnir, D., O. Biham, D. Lidar, and O. Malcai, "Is the Geometry of Nature Fractal?," *Science*, **278**, 39–40 (1998).

Ball, P.C. and R. Evans, "Temperature Dependence of Gas Adsorption on a Mesoporous Solid: Capillary Criticality and Hysteresis," *Langmuir*, **5**, 714–723 (1989).

Barker, J.A., R.O. Watts, J.K. Lee, T.P. Schafer, and Y.T. Lee, "Interatomic Potentials for Krypton and Xenon," *J. Chem. Phys.*, **61**, 3081–3089 (1974).

Bojan, M.J. and W.A. Steele, "Computer Simulations of Sorption in Model Cylindrical Pores," in *Proceeding of Fundamental of Adsorption*, M.D. LeVan (Eds.), pp. 17–33, Kluwer Academic Publishers, Boston, 1996.

Burgess, C.G.V., D.H. Everett, and S. Nuttal, "Adsorption of CO_2 and Xenon by Porous Glass over a Wide Range of Temperature and Pressure: Applicability of the Langmuir Case VI Equation," *Langmuir*, **6**, 1734–1738 (1990).

Celestini, F., "Capillary Condensation Within Nanopores of Various Geometries," *Physics Lett. A*, **228**, 84–90 (1997).

Gelb, L.D. and K.E. Gubbins, "Characterization of Porous Glasses: Simulation Models, Adsorption Isotherms and the BET Analysis Method," *Langmuir*, **14**, 2097–2111 (1998).

Kierlick, E., M.L. Rosinberg, G. Tarjus, and E. Pitard, "Mean-Spherical Approximation for a Lattice Model of a Fluid in a Disordered Matrix," *Mol. Phys.*, **95**, 341–352 (1998).

Landmesser, H., H. Kosslick, W. Storek, and R. Frick, "Interior Surface Hydroxyl Groups in Ordered Mesoporous Silicates," *Solid State Ionics*, **101–103**, 271–277 (1997).

Levitz, P., "Off-Lattice Reconstruction of Porous Media: Critical Evaluation, Geometrical Confinement and Molecular Transport," *Adv. Coll. Int. Sci.*, **76–77**, 71–106 (1998).

Levitz, P., G. Ehret, S.K. Sinha, and J.M. Drake, "Porous Vycor Glass: The Microstructure as Probed by Electron Microscopy, Direct Energy Transfer, Small-Angle Scattering and Molecular Adsorption," *J. Chem. Phys.*, **95**, 6151–6161 (1991).

Levitz, P., V. Pasquier, and I. Cousin, "Off-Lattice Reconstructed Biphasic Media Using Gaussian Random Field: Evaluation for Different Disordered Porous Solids," *Caracterization of Porous Solids IV*, B. Mc Enanay, T.J. May, J. Rouquerol, K.S.W. Sing, and K.K. Unger (Eds.), p. 213, The Royal Soc. of Chem., London, 1997.

Levitz, P. and D. Tchoubar, "Disordered Porous Solids: From Chord Distributions to Small Angle Scattering," *J. Phys. I*, **2**, 771–790 (1992).

Mason, G., "Detemination of the Pore-Size Distributions and Pore-Space Connectivity of Vycor Porous Glass from Adsorption-Desorption Hysteresis Capillary Condensation Isotherms," *Proc. R. Soc. Lond. A*, **415**, 453–486 (1988).

Mitropoulos, A.C., J.M. Haynes, R.M. Richardson, and N.K. Kanellopoulos, "Characterization of Porous Glass by Adsorption of Dibromomethane in Conjunction with Small Angle Scattering," *Phys. Rev. B.*, **52**, 10035–10042 (1995).

Morishige, K., H. Fujii, M. Uga, and D. Kinakawa, "Capillary Critical Point of Argon, Nitrogen, Oxygen, Ethylene and Carbon Dioxide in MCM41," *Langmuir*, **13**, 3494–3498 (1997).

Nicholson, D. and N.G. Parsonage, *Computer Simulation and the Statistical Mechanics of Adsorption*, Academic Press, 1982.

Nuttal, S., "Adsorption and Capillary Condensation of Xenon in Porous Glass and Porous Carbon," PhD thesis, University of Bristol, UK (1974).

Page, J.H., J. Liu, A. Abeles, E. Herbolzheimer, H.W. Deckman, and D.A. Weitz, "Adsorption and Desorption of a Wetting Fluid in Vycor Studied by Acoustic and Optical Techniques," *Phys. Rev. E.*, **52**, 2763–2777 (1995).

Page, K.S. and P.A. Monson, "Monte Carlo Simulation of Phase Diagrams for a Fluid Confined in a Desordered Porous Material," *Phys. Rev. E*, **54**, 6557–6564 (1996).

Pellenq, R.J.-M. and P. Levitz, to be published.

Pellenq, R.J.-M. and D. Nicholson, "Intermolecular Potential Function for the Physical Adsorption of Rare Gases in Silicalite," *J. Phys. Chem.*, **98**, 13339–13349 (1994).

Pellenq, R.J.-M. and D. Nicholson, "Grand Canonical Monte-Carlo Simulation of Adsorption of Small Molecules in Silicalite Zeolite," *Langmuir*, **11**, 1626–1635 (1995).

Pellenq, R.J.-M., B. Tavitian, D. Espinat, and A. Fuchs, "Grand Canonical Monte-Carlo Simulations of Adsorption of Polar and Non Polar Molecules in NaY Zeolite," *Langmuir*, **12**, 4768–4783 (1996).

Peterson, B.K. and K.E. Gubbins, "Phase Transitions in a Cylindrical Pore, Grand Canonical Monte-Carlo, Mean Field Theory and the Kelvin Equation," *Mol. Phys.*, **62**, 215–226 (1987).

Rouquerol, F., J. Rouquerol, and K. Sing, *Adsorption by Powders and Porous Solids*, Academic Press, 1998.

Torii, R.H., K.J. Maris, and G.M. Seidel, "Heat Capacity and Torsional Oscillator Studies of Molecular Hydrogen in Porous Vycor Glass," *Phys. Rev. B*, **41**, 7167–7181 (1990).